Journal of Catalysis **199,** 328–337 (2001)
doi:10.1006/jcat.2001.3178, available online at http://www.idealibrary.com on IDEAL®

Partial Oxidation of Methane on Silica-Supported Different Alkali Metal Molybdates

A. Erdőhelyi,[1] K. Fodor, R. Németh, A. Hancz, and A. Oszkó

Institute of Solid State and Radiochemistry, University of Szeged, and Reaction Kinetics Research Group of the Hungarian Academy of Sciences, P.O. Box 168, H-6701, Szeged, Hungary

Received October 12, 2000; revised December 12, 2000; accepted January 12, 2001; published online March 27, 2001

The partial oxidation of methane was studied on silica-supported alkali metal molybdate catalysts in a fixed-bed continuous-flow reactor at 860–923 K using O_2 as oxidant. The catalysts were characterized by Raman and XP spectroscopy. It was found that the surface structure and composition of molybdates deposited by impregnation depend on the cation. From lithium to potassium monomolybdate was formed with the original structure, Rb_2MoO_4/SiO_2 contains distorted $[MoO_4]$ tetrahedra, and in the case of cesium dimolybdate was obtained. The main products of the oxidation reaction were formaldehyde, ethane, CO, and CO_2. The activity of the catalysts and the product distribution were markedly influenced by the structure of the catalysts. The highest catalytic activity was measured on Rb_2MoO_4/SiO_2. Formaldehyde in a larger quantity was produced on MoO_3/SiO_2, but when the rate was related to the amount of surface molybdenum atoms Rb_2MoO_4/SiO_2 had the highest activity. A possible mechanism for the oxidation of methane is discussed.

Key Words: **partial oxidation of methane; alkali metal molybdate; Raman spectra of alkali metal molybdates.**

1. INTRODUCTION

The partial oxidation of methane to oxygenates over MoO_3-based oxides has been studied extensively. The silica-supported sample was found to be one of the most active and selective catalysts (1–4). When oxygen was used as oxidant formaldehyde was obtained as the main product (1–3). In the presence of N_2O, methanol formation with relatively high selectivity was also observed (4).

Supported MoO_3 was active and selective in the oxidative dehydrogenation of ethane to give ethylene and acetaldehyde. However, a better catalytic performance was obtained when alkali metal molybdates were used as catalysts (5, 6).

The catalytic effect of alkali metal molybdates in the methane conversion has not yet been well explored. In the oxidative coupling of methane the good catalytic activity of K_2MoO_4 has been reported (7). K_2MoO_4/ZSM-5 was also proved to be active in the conversion of methane into benzene under nonoxidative conditions (8). Recently the partial oxidation of methane was studied on K_2MoO_4 deposited on various supports (9). It was found that the structure of the molybdates on the surface of the support depended sensitively on the pH value of the slurry. At low pH a significant amount of $K_2Mo_2O_7$ was formed. Formaldehyde in a larger quantity was produced on a silica-supported catalyst containing a greater amount of $K_2Mo_2O_7/SiO_2$ and of K_2MoO_4/ZSM-5. Adding 2% Na to 7% MoO_3/SiO_2 sample significantly increased the CH_4 conversion and the $HCHO + CH_3OH$ yield at 507 kPa pressure (10).

In contrast to these observations it has been shown that alkali metal impurities lead to the formation of alkali metal molybdates which have a negative effect on the conversion of methane to formaldehyde (11). A kinetic model has been proposed to account for the poisoning of MoO_3/SiO_2 by sodium. The effects of Na, K, and Cs additives on both the structure of MoO_3/SiO_2 and its behavior as a catalyst for selective oxidation of methane to formaldehyde were also investigated (12). Addition of alkali metals decreased the number of isolated surface molybdenum oxide species and formed new alkali metal compounds. The oxygen associated with the alkali metal molybdenum compounds was generally not available for oxidation reaction. Consequently, the alkali metal addition decreased the catalytic activity for methane oxidation (12). Marchi *et al.* (13) also found that the pre-impregnation of silica support with sodium strongly diminishes the Mo=O concentration due to the formation of $Na_2Mo_2O_7$ species and tetrahedral monomers with a high degree of symmetry. As a result of these modifications both methane formation and formaldehyde formation are strongly inhibited.

The present paper gives an account of the selective oxidation of methane with oxygen on silica-supported alkali metal molybdates. Attention is paid to the characterization of the species formed on the surface of the catalysts, and to the effect of the alkali metal on the product distribution of the reaction.

[1] To whom correspondence should be addressed. Fax: 36-62-424-997. E-mail: erdohely@chem.u-szeged.hu.

0021-9517/01 $35.00

2. EXPERIMENTAL

Materials. The catalysts were prepared by impregnating the SiO_2 support (Cab-O-Sil) with a basic solution (pH ~11) of ammonium molybdate [$(NH_4)_6Mo_7O_{24} \times 4H_2O$] or different alkali metal molybdates, M_2MoO_4 (M = Li, Na, K (Aldrich), Rb, Cs), to yield a nominal 2% loading of MoO_3 (6). When a decrease in the pH value was observed during the impregnation it was restored with NH_4OH solution to pH 11. The suspension was dried at 373 K and calcined at 863 K for 5 h. The rubidium and cesium molybdates were prepared from rubidium and cesium carbonates (Aldrich) and MoO_3 (Aldrich) (14). MoO_3 was stirred into the hot solution of the calculated amount of alkali metal carbonate until it dissolved. The solution was filtered and the alkali metal molybdates were crystallized. All catalysts will be denoted by the formula as monomolybdate independent of the structure formed during the preparation.

Before catalytic measurements, each catalyst was oxidized in an O_2 stream for 1 h at 773 K in the reactor; the catalyst was then flushed with He and heated to the reaction temperature in flowing He.

The reactant gases, CH_4 (99.995%) and O_2 (99.99%), were used as received. He (99.996%) was purified with an oxy-trap.

Methods. The reactions were carried out in a fixed-bed continuous-flow reactor made of quartz (100 × 27 mm o.d.) which was connected to a capillary tube (2 mm i.d.) so that the products could be rapidly removed from the heated zone. The reactor was heated by an external oven. A small glass tube containing a thermocouple was placed in the middle of the catalyst bed. Generally 0.5 g of sample was used as catalyst. The dead volume of the reactor was filled with quartz beads. The reacting gas mixture usually consisted of 90% CH_4 and 10% O_2. The flow rate of the reactants was usually 47 ml/min and the space velocity was 5640 h^{-1}.

The gases were analyzed by gas chromatography (Chrompack 9001) by thermal conductivity and flame ionization detectors. The separation of the products was accomplished with a Carboxen 1000 column (Supelco) (1/8 in. × 5 ft). The formaldehyde standards for the calibration curves were prepared by dissolving paraformaldehyde and analyzed by Romijn's iodometric titration method (15).

The conversion and selectivity for reaction products, S_i, were defined as

$$\text{Conversion} = \frac{\sum x_i n_i}{x_{CH_4} + \sum x_i n_i}$$

$$\text{Selectivity } S_i = \frac{x_i n_i}{\sum x_i n_i},$$

where x_i and x_{CH_4} are the mole fraction of product i and CH_4, respectively, and n_i is the number of carbon atoms in each molecule of product i.

A pulse reactor was also employed (8-mm-i.d. quartz tube). The products were analyzed by an online mass spectrometer (Balzers QMS 200). Usually 0.3 g of sample was used and the dead volume of the reactor was filled with quartz beads. One pulse contained 20.8 μmol of gas.

The Raman spectra of the clean and the silica-supported molybdenum oxides and alkali metal molybdates were recorded by using a Bio-Rad FT-Raman spectrometer. The Raman spectrometer system possessed a Spectra-Physics T 10-106 c Nd:YVO_4 laser. It was tuned to the exciting line at 1064 nm. The radiation intensity was 540 mW. A liquid-nitrogen-cooled Ge detector was used. In the case of silica-supported samples 4096 scans resulted in a sufficient signal-to-noise ratio.

XPS measurements were performed in a Kratos XSAM 800 instrument at a base pressure of 5×10^{-9} Torr using Mg$K\alpha$ (1253.6 eV) primary radiation (14 kV, 15 mA) (9). To compensate for possible charging effect, binding energies were normalized with respect to the position of the Si 2p line in SiO_2; this value was assumed constant at 103.4 eV. The pass energy was set at 40 eV and an energy step width of 50 meV and dwell time of 300 ms were used. Typically 10 scans were accumulated for each spectrum.

The BET surface areas of the catalysts were measured by N_2 adsorption at 77 K in a conventional volumetric apparatus.

3. RESULTS

3.1. Characterization of Catalysts

XP spectra. The photoelectron spectra of MoO_3 and alkali metal molybdates showed the characteristic Mo 3d doublet. The binding energy of the Mo 3$d_{5/2}$ peak was the highest in the MoO_3 (233.0 eV) and it shifted to lower energies from Li_2MoO_4 (232.7 eV) to Rb_2MoO_4 and Cs_2MoO_4 (231.8 eV) (Fig. 1). The binding energy of the O 1s peak in MoO_3 was 530.8 eV. This value shifted to lower energy in the case of alkali metal molybdates, and it was 530.6 eV for Li_2MoO_4, but from K_2MoO_4 to Cs_2MoO_4 530 eV was detected. The characteristic binding energies of the alkali metals in the alkali metal molybdates were almost the same as those in the different alkali metal salts. For example, the feature apparent around 238.5 eV in the XP spectrum of rubidium molybdate samples (Figs. 1 and 2) originates from the Rb 3$p_{3/2}$ orbital. Some characteristic XPS data are collected in Table 1.

The binding energy of the Mo 3$d_{5/2}$ peak in silica-supported catalysts was nearly the same in all cases (232.4–232.0 eV). These values were somewhat lower for MoO_3 and for Li_2MoO_4, but for potassium, rubidium, and cesium molybdates higher values were observed (Fig. 2) as compared to those for unsupported alkali metal molybdates. In the case of Rb_2MoO_4/SiO_2 a small peak was detected at

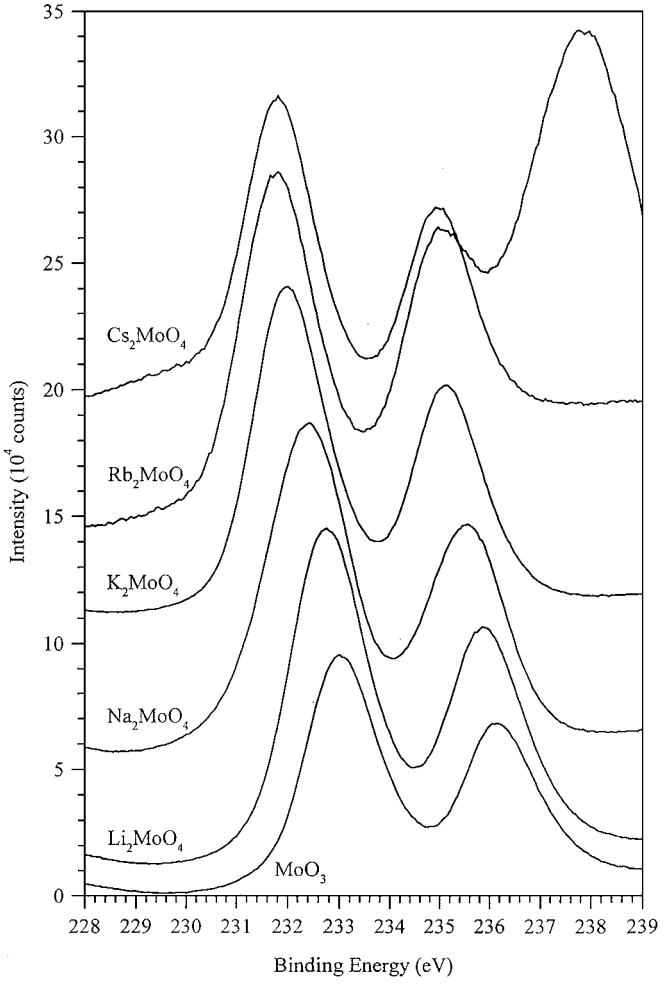

FIG. 1. XP spectra of MoO_3 and different alkali metal molybdates.

about 229 eV. This is a satellite peak of Rb $3p_{3/2}$ produced by Al$K\alpha_{3,4}$ radiation, because we used a nonmonochromatic X-ray source.

Table 1 contains the peak area ratios of the Mo 3*d* and Si 2*p* peaks for different silica-supported samples. As the detection depth of the X-ray photoelectron spectroscopy technique is limited to less than 2–4 nm from the surface, the atomic ratios determined by XPS represent information on the surface layer, or on just the few top layers of the samples. Therefore, the ratios of the peak areas, taking into account the sensitivity factor of the individual peaks, can be regarded as the surface atomic ratios. The data suggest that the amount of surface Mo atoms is the highest in cesium molybdate supported on silica and it decreases in the following order: $MoO_3/SiO_2 > K_2MoO_4/SiO_2 > Na_2MoO_4/SiO_2 \geq Li_2MoO_4/SiO_2 > Rb_2MoO_4/SiO_2$. On MoO_3/SiO_2 the number of surface Mo atoms is about 3 times higher than that on Rb_2MoO_4/SiO_2 (Table 1).

TABLE 1

Some Characteristic XPS Data of Different Alkali Metal Molybdates

	Clean, Binding energy (eV)			Silica-supported samples Binding energy (eV)			
	Mo^{6+}		O^{2-}	Mo^{6+}		O^{2-}	Mo 3*d*/Si 2*p* peak area ratio[a]
Sample	$3d_{5/2}$	$3d_{3/2}$	1*s*	$3d_{5/2}$	$3d_{3/2}$	1*s*	
MoO_3	233.0	236.1	530.8	232.4	234.8	533.1	0.0078
Li_2MoO_4	232.7	235.9	530.6	232.4	235.5	532.9	0.0035
Na_2MoO_4	232.4	235.6	530.3	232.4	235.6	532.8	0.0036
K_2MoO_4	232.0	235.1	530	232.4	235.2	532.8	0.0054
Rb_2MoO_4	231.8	235.0	530	232.0	235.2	532.9	0.0026
Cs_2MoO_4	231.8	234.9	530	232.0	235.1	532.9	0.0091

[a] Taking into account the sensitivity ratio of the given peaks.

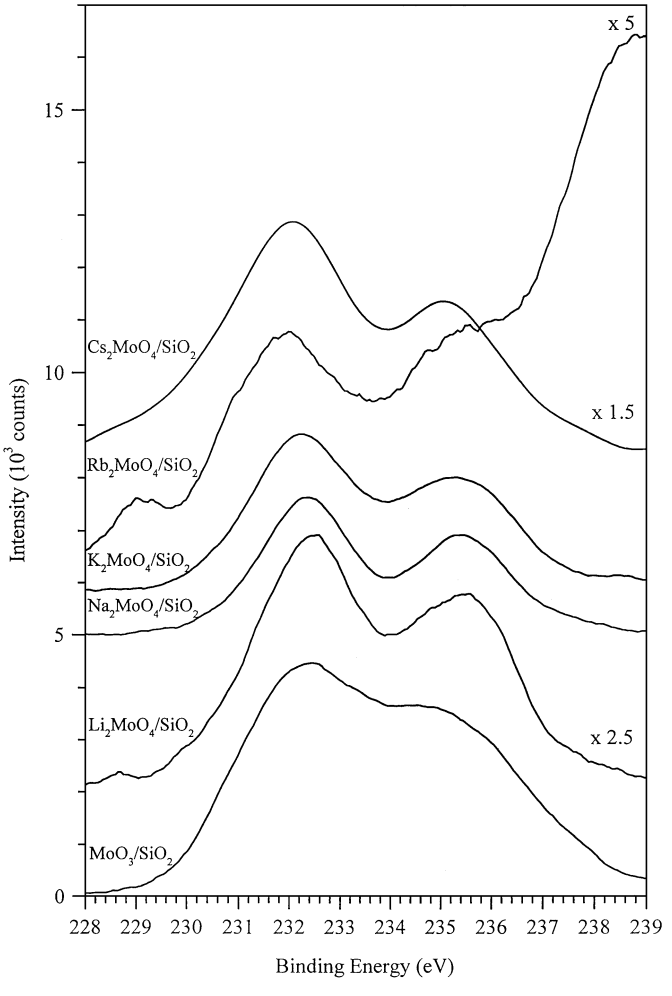

FIG. 2. XP spectra of SiO_2-supported MoO_3 and different alkali metal molybdates.

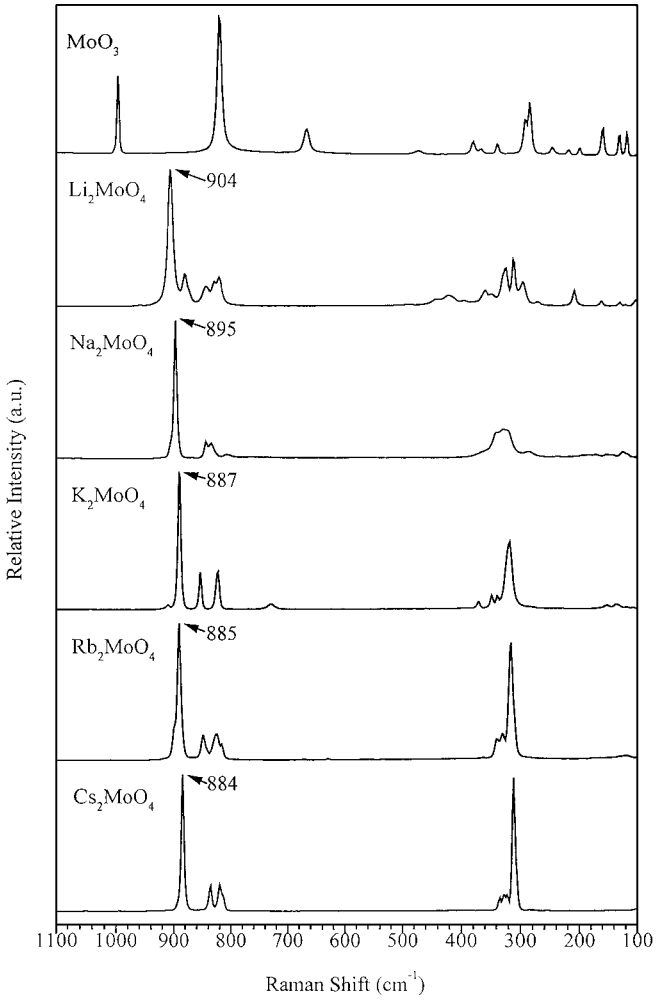

FIG. 3. Laser Raman spectra of MoO_3 and different alkali metal molybdates.

Raman spectra. The Raman spectra of crystalline alkali metal molybdates as raw materials, in comparison with the spectrum of molybdenum oxide, are displayed in Fig. 3. The positions of the main Raman shifts are shown in Table 2. The Raman frequencies of unsupported clean MoO_3 (16) and those of alkali metal molybdates, such as Li_2MoO_4 (21), Na_2MoO_4 (12, 17, 22), K_2MoO_4 (12, 18, 22), and Cs_2MoO_4 (12), agree very well with those reported earlier. The figure clearly shows that the ν_s frequency of the Mo–O band in the alkali metal molybdates continuously shifted from Li_2MoO_4 (904 cm^{-1}) to Cs_2MoO_4 (884 cm^{-1}).

When Li_2MoO_4 and Na_2MoO_4 were supported on SiO_2, nearly the same Raman spectra were recorded as mentioned above. In the case of potassium, rubidium, and cesium molybdates new bands appeared on the spectra at 928–936 cm^{-1} and with the exception of the last sample at 908–912 cm^{-1} (Fig. 4).

BET surface area. The BET surface area of the SiO_2 (198 m^2/g)-supported alkali metal molybdate catalysts first decreased with an increase in the cation size, Li_2MoO_4/SiO_2 (111 m^2/g) > Na_2MoO_4/SiO_2 (69 m^2/g), and then increased, K_2MoO_4/SiO_2 (76 m^2/g) < Rb_2MoO_4/SiO_2 (120 m^2/g) and Cs_2MoO_4/SiO_2 (110 m^2/g). The decrease in the BET surface area in the case of K_2MoO_4/SiO_2 (23) and different alkali metal molybdate silica samples (6) was observed earlier.

3.2. Oxidation of Methane on Silica-Supported Alkali Metal Molybdates

The reaction was carried out at 923 K and the inlet gas contained 90% CH_4 and 10% O_2. The main products of the reaction were formaldehyde, ethane, carbon monoxide, carbon dioxide, and water. Traces of methanol and ethylene were also detected. For comparison the effect of MoO_3/SiO_2 was also studied.

The initial conversion of methane decreased in the order $Rb_2MoO_4/SiO_2 > Cs_2MoO_4/SiO_2 > K_2MoO_4/SiO_2 =$

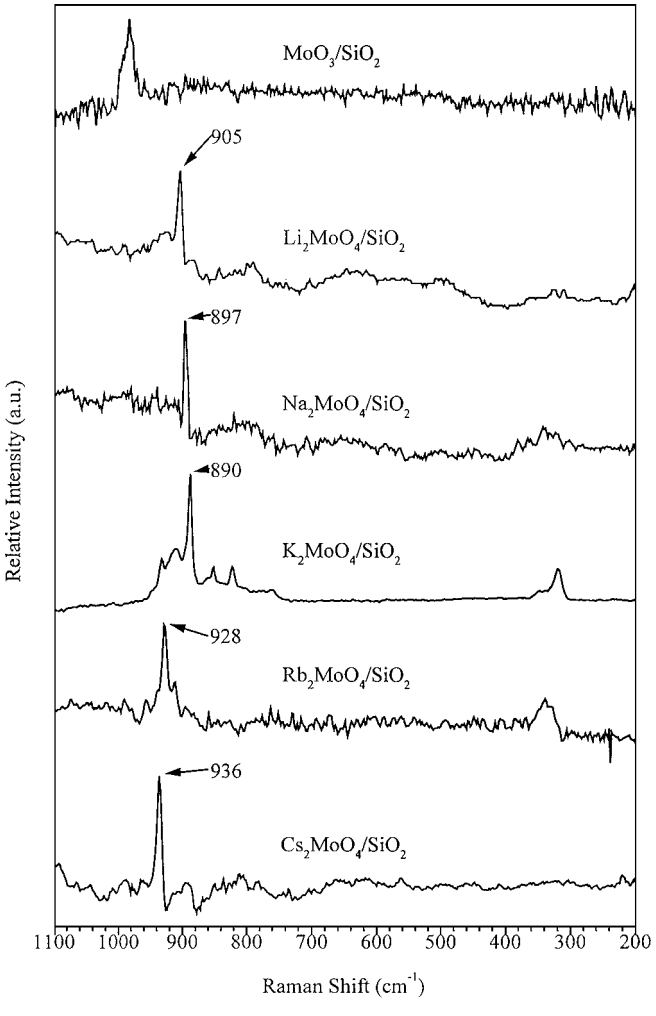

FIG. 4. Laser Raman spectra of SiO_2-supported MoO_3 and different alkali metal molybdates.

TABLE 2

Main Raman Frequencies[a] of MoO_3 and Different Alkali Metal Molybdates

MoO_3		Li_2MoO_4,	Na_2MoO_4		K_2MoO_4		Rb_2MoO_4,	Cs_2MoO_4,	$K_2MO_2O_7$,	$(NH_4)_2MO_2O_7$,
This work	(16)	This work	(17)	This work	This work	(18)	This work	This work	(19)	(20)
995 (s)	994	904 (vs)	897	895 (vs)	902 (vw)	922	901 (sh)	884 (vs)	929	937
819 (vs)	820	879 (w)	843	842 (w)	887 (vs)	904	885 (vs)	836 (s)	908	910
666 (w)	665	842 (w)	836	834 (w)	851 (s)	885	840 (w)	816 (sh)	873	720
379 (vw)	382	828 (w)		327 (s)	821 (s)	849	818 (sh)	819 (s)	860	456
337 (vw)	338	819 (w)			729 (vw)	819	821 (w)	334 (w)		365
283 (s)	292, 285	358 (vw)			369 (vw)	710	339 (w)	327 (w)		291
		323 (w)			347 (vw)		333 (w)	322 (w)		
		310 (w)			316 (vs)		315 (vs)	311 (vs)		
		295 (vw)								

[a] Intensity: vs, very strong; s, strong; w, weak; vw, very weak; sh, shoulder.

$Na_2MoO_4/SiO_2 > MoO_3/SiO_2 > Li_2MoO_4/SiO_2$ (Fig. 5). During the conditioning period at 923 K, i.e., in the first hours of the reaction (Fig. 5), significant decay of the methane conversion and of the products formation occurred. The exception was MoO_3/SiO_2; in this case the conversion did not change considerably. For example, on Cs_2MoO_4/SiO_2 the initial CH_4 conversion was 4.0% but after 180 min of reaction it was only 1.08%. Some characteristic data of the reaction are summarized in Table 3. The conversion of methane varied in the steady state between 1.0–4.6 % on the different alkali metal molybdates. It decreased in the following sequence: $Rb_2MoO_4/SiO_2 > MoO_3/SiO_2 > K_2MoO_4/SiO_2 > Cs_2MoO_4/SiO_2 = Na_2MoO_4/SiO_2 = Li_2MoO_4/SiO_2$. The conversion of oxygen changed in the same way as the methane consumption; it was the highest in the steady state at 923 K on rubidium molybdate silica (65.6%) and the lowest on Li_2MoO_4/SiO_2 (12.6%).

The selectivities for HCHO formation at 923 K were the highest on MoO_3/SiO_2 (33.4%) and Li_2MoO_4 (24.3%). The

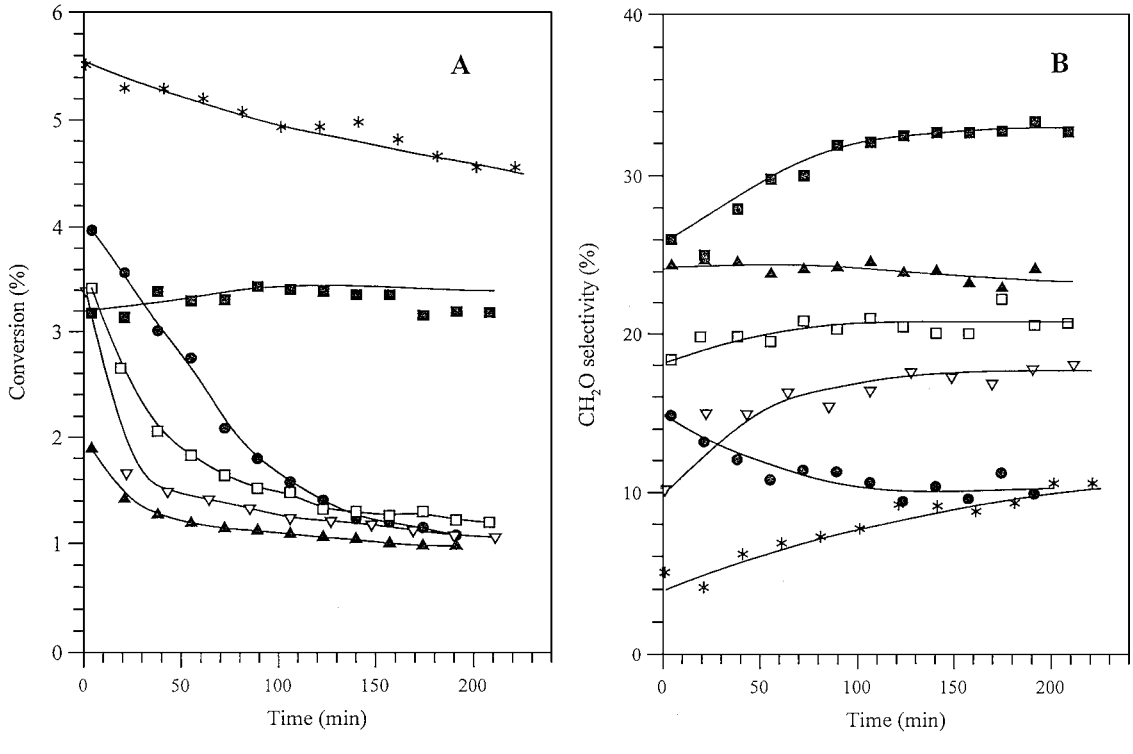

FIG. 5. Conversion of methane (A) and selectivity of HCHO formation (B) on SiO_2-supported Li_2MoO_4 (▲), Na_2MoO_4 (▽), K_2MoO_4 (□), Rb_2MoO_4 (✱), Cs_2MoO_4 (●), and MoO_3 (■) catalysts at 923 K.

TABLE 3

Some Characteristic Data of the $CH_4 + O_2$ Reaction at 923 K on Different Silica-Supported Alkali Metal Molybdate Catalysts[a]

Catalysts	CH_4 conv., %	Rate of product formation, nmol/g · s				Selectivity of product formation, %			
		HCHO	CO	CO_2	C_2	HCHO	CO	CO_2	C_2
MoO_3/SiO_2	3.2	423.6	405.4	397.8	27.2	33.4	31.4	30.7	4.3
Li_2MoO_4/SiO_2	1.0	92.8	198.7	67.8	11.8	24.3	51.8	17.7	6.3
Na_2MoO_4/SiO_2	1.1	87.7	226.5	161.7	6.9	17.9	46.2	33.0	2.8
K_2MoO_4/SiO_2	1.2	86	216	96	8.8	20.7	51.6	23.3	4.3
Rb_2MoO_4/SiO_2	4.6	213.2	667	963	83.3	10.6	33.2	47.9	8.3
Cs_2MoO_4/SiO_2	1.1	41.6	284.3	161.2	18.2	9.9	42.8	38.5	8.7

[a] The data were obtained after 180 min of reaction.

lowest HCHO selectivity was obtained on Cs_2MoO_4/SiO_2 (9.9%) (Fig. 5) although on this sample the CH_4 conversion was one of the lowest. From these results it seems that in the case of alkali metal molybdates there is no direct connection between the HCHO selectivity and the CH_4 conversion.

A significant amount of C_2H_6 was also formed in the reaction; the selectivity changed between 2.8–8.7% (Table 3).

The temperature dependence of the reaction was studied in the range of 863–923 K. The conversion varied between 4.6% and 0.1%. The lowest conversion was observed on Li_2MoO_4/SiO_2 (Fig. 6). The selectivity for HCHO formation increased with decreasing temperature in all cases. At 863 K the selectivity of HCHO formation on Na_2MoO_4/SiO_2 and on MoO_3/SiO_2 was about 55% (Fig. 6) although the CH_4 conversion was only 0.3% and 0.4%, respectively. The C_2 selectivity changed oppositely: it increased with increasing temperature in all cases. The CO and CO_2 selectivities were enhanced or did not change with increasing temperature with the exception of Rb_2MoO_4/SiO_2 and Cs_2MoO_4/SiO_2 catalysts. In these cases the CO selectivity slightly decreased with increasing temperature.

The effect of the pure SiO_2 used as support in this study was also examined under the same experimental conditions as those previously described. It was found that the methane conversion was below 0.25% at 923 K in all cases.

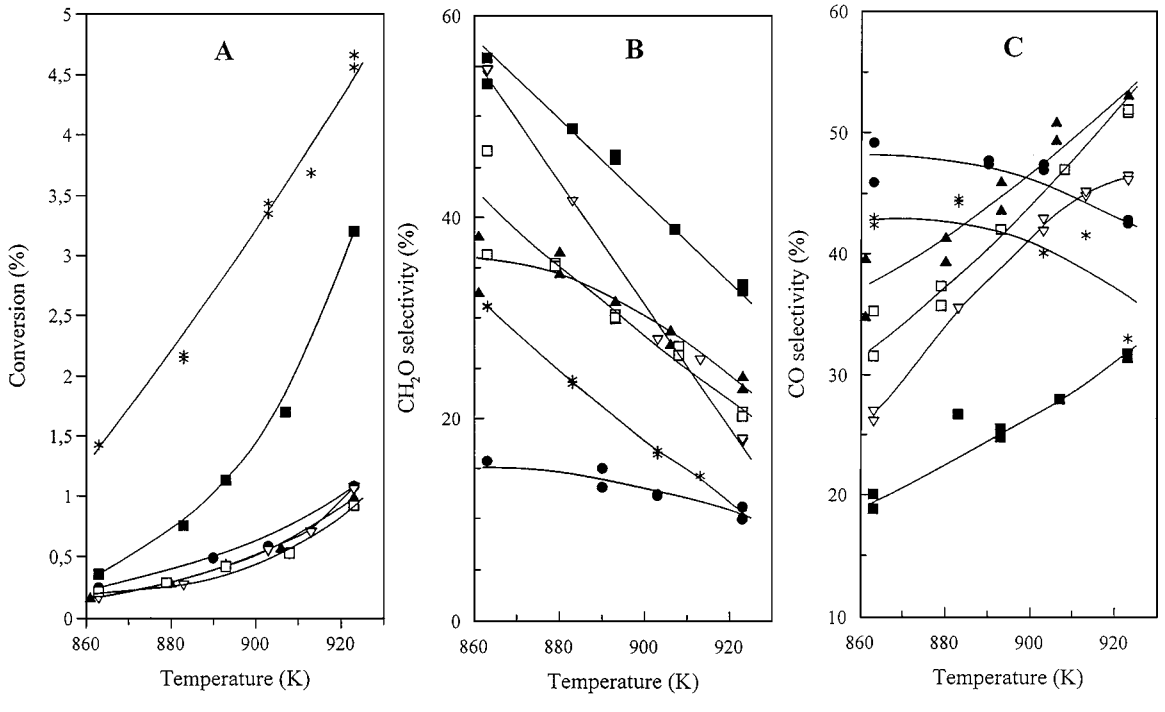

FIG. 6. Effect of the temperature on the methane conversion (A), on selectivity of HCHO (B), and on CO formation (C) on SiO_2-supported Li_2MoO_4 (▲), Na_2MoO_4 (▽), K_2MoO_4 (□), Rb_2MoO_4 (✱), Cs_2MoO_4 (●), and MoO_3 (■) catalysts.

3.3. Pulse Experiments

In the subsequent measurements the interaction of the catalysts with methane and the reaction were investigated by the pulse technique on Rb_2MoO_4/SiO_2 at 923 K. Only a small amount of H_2, HCHO, CO, and CO_2 and traces of C_2H_6 formed when CH_4 was admitted onto the catalyst in a He stream. The methane conversion was below 0.8% in the first pulse and the amount of products slightly decreased as a function of pulse number. After seven methane pulses (145.6 μmol of CH_4) the catalyst was treated with O_2 and a small amount of (1.8 μmol/g catalyst) CO_2 formation was observed. The O_2 consumption was higher (about 1.2 μmol/g) than required for the CO_2 formation. From this result it can be calculated that about 10% of Mo^{6+} was reduced to Mo^{5+}.

When the sample was held in a CH_4 stream at 923 K and O_2 pulses (20.8 μmol) were introduced to the catalyst the main products were CO_2, and CO, and small amounts of HCHO, H_2, and C_2H_6 were also detected (Fig. 7A). The O_2 conversion was about 56% in the first pulse and it did not change in the subsequent pulses. After O_2 injection the carrier gas was changed to He, the sample was flushed with it, and O_2 pulses were given again, and about 2 μmol of CO_2 was formed.

On injection of CH_4 into the O_2 stream onto the Rb_2MoO_4/SiO_2 at 923 K the amount of CO_2 formed was about one-third, and that of CO was about one-half that in the previous case when O_2 was let into the CH_4 flow, but the same amount of H_2 and HCHO could be detected; C_2H_6 was not observed (Fig. 7B). The CH_4 conversion was only 17% in the first pulse. The CO_2 to CO ratio when O_2 let given in the CH_4 stream was more than 2, but when CH_4 was injected into O_2 this ratio was much lower, about only 1 (Fig. 7).

When $CH_4 + O_2$ (9 : 1) pulses were introduced onto the catalyst at 923 K and He was the carrier gas the methane conversion was only 4.5% in the first pulse and it slightly decreased as a function of pulse number, while the amount of CO_2 formed also decreased. The CO_2 to CO ratio in the reaction was about 1 in this case, too (Fig. 7C).

3.4. Examination of the Used Catalysts

In order to establish changes on the catalyst surface the reaction was interrupted and the catalysts were examined. After the catalytic run the samples were treated with O_2 at 923 K and the O_2 consumption and CO_2 formation—produced in the oxidation of surface carbon—were followed. After 1 h of reaction we found only trace amounts of carbon ($\sim$0.01 μmol/g) on Rb_2MoO_4/SiO_2. The oxygen consumption was, however, higher than that required for the CO_2 formation. Taking into account the O_2 uptake about 10% of the Mo^{6+} reduced to Mo^{5+}. Note that the color of the catalyst remained white during the catalytic reaction (the reduced sample is dark blue).

XPS analysis of the used sample showed only slight changes in the binding energies of Mo 3*d* peaks. They were about 0.1 eV lower than in the case of unused catalyst. The Mo to Si ratio was lower than the same value for the unused sample (Table 1). In the case of Rb_2MoO_4/SiO_2 it was only 0.00073.

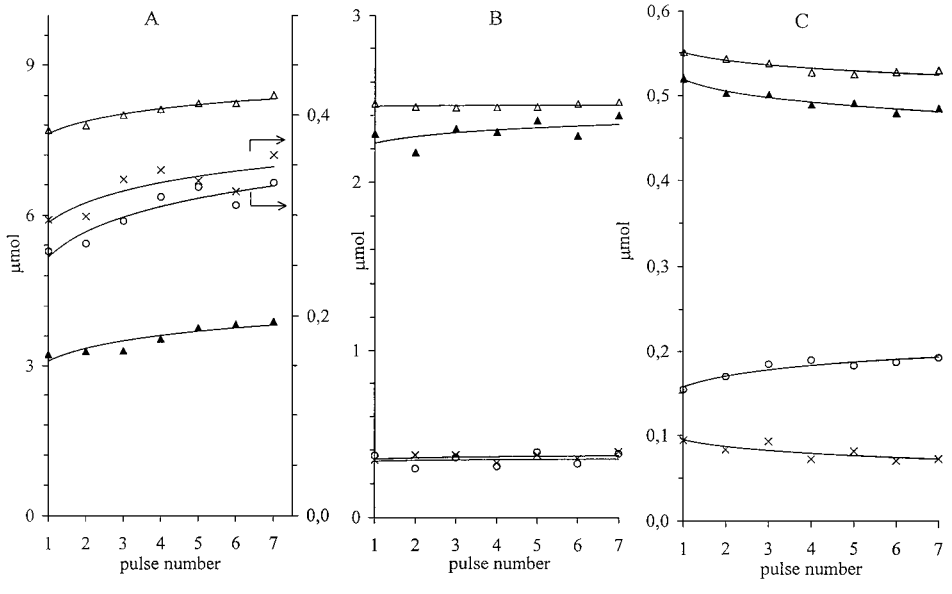

FIG. 7. Amount of CO_2 (Δ), CO (▲), H_2 (×), and HCHO (○) formed in O_2 pulses into CH_4 flow (A), in CH_4 pulses into O_2 stream (B), and in $CH_4 + O_2$ pulses into He stream (C), at 923 K on Rb_2MoO_4/SiO_2 catalyst.

The Raman spectra of the used samples were practically the same as those of the unused catalysts; only the peak intensity decreased.

4. DISCUSSION

4.1. Some Properties of Alkali Metal Molybdates

As supported MoO_3 has been widely used as a catalyst, detailed measurements have been performed for its surface characterization. Less attention has been paid so far to supported and unsupported alkali metal molybdates.

The alkali metal monomolybdates contain MoO_4 tetrahedra (24), the structure of Li_2MoO_4 is phenacite (25), while Na_2MoO_4 has a spinel structure (26). K_2MoO_4 and Rb_2MoO_4 are monoclinic (24, 27) and Cs_2MoO_4 is orthorhombic (27, 28).

The Raman frequencies of unsupported alkali metal molybdates as Table 2 shows agree well with those determined before. The Raman bands in the 930–850 cm^{-1} region are attributed to the symmetric and asymmetric stretching modes of the terminal Mo=O bond. The bands around 310–370 cm^{-1} are the corresponding bending modes of the terminal Mo=O bond (9, 20). From Fig. 3 and Table 2 it can be seen that the ν_s frequency of the Mo–O band shifted toward lower wavenumbers from Li_2MoO_4 (904 cm^{-1}) to Cs_2MoO_4 (884 cm^{-1}). For the explanation of this shift the observation of Hardcastle and Wachs (20) has to be taken into account. A correlation was developed for relating Raman stretching frequencies of molybdenum–oxygen (Mo–O) bonds to their respective bond distances in molybdenum oxide compounds: $\nu = 32895e^{-2.073R}$ where ν is the Raman frequency in inverse centimeters and R is the bond distance in angstroms (20). If the Mo–O bond distances are calculated using this equation from the Raman frequencies obtained in our cases (Table 2) the results are in good correlation—except for Cs_2MoO_4—with the data found in the literature (1.752, 1.768, and 1.781 Å for Na_2MoO_4 (17), 1.76 Å for K_2MoO_4 (24), and 1.792 Å for Cs_2MoO_4 (28)) taking into account the standard deviation of this method (± 0.016 Å). So the observed Raman shifts can be explained with the different Mo–O bond lengths in the different alkali metal molybdates.

The XP spectra of alkali metal monomolybdates (Fig. 1) show that the binding energy of the Mo $3d_{5/2}$ peak shifted from 233.0 eV (MoO_3) to 231.8 eV (Cs_2MoO_4). The observed shift in the binding energies means that the Mo–O bond strength changes depending on the cations and consequently—as the Raman results reveal—so does the Mo–O bond length.

When the molybdates were supported on silica nearly the same XP spectra were recorded in all cases. The binding energies of the Mo $3d_{5/2}$ peaks in MoO_3 and in Li_2MoO_4 shifted to lower values but in the cases of K-, Rb-, and Cs_2MoO_4 higher values were detected. These results clearly show that in the silica-supported alkali metal molybdate samples the effect of the cation on the molybdenum is strongly diminished. The decrease in the difference of Mo $3d_{5/2}$ and Mo $3d_{3/2}$ binding energies in MoO_3/SiO_2 samples (Table 1) is the result of the simultaneous existence of Mo in different oxidation states on the surface of the catalyst, i.e., the MoO_3/SiO_2 reduced in vacuum.

The Raman spectra of MoO_3/SiO_2, Li_2MoO_4/SiO_2, and Na_2MoO_4/SiO_2 are nearly the same as was observed in the case of unsupported compounds (Figs. 3 and 4). It means that these molybdates are bonded to the surface in the original structure. In the other cases new Raman shifts were detected on the dried and calcined samples.

The characteristic features of the Raman spectra of supported K_2MoO_4/SiO_2 were described earlier (9, 23). It was found (these new Raman shifts appeared at 931 and 908 cm^{-1}) that the composition and the structure of molybdates deposited by impregnation depended sensitively on the pH value of the slurry containing the support. The pH value decreased during the impregnation and if it was not restored to pH 11 a significant amount of $K_2MO_2O_7$ was formed (9). Verbruggen *et al*. studied the effect of K on the structure of calcined molybdenum catalysts prepared by the impregnation of SiO_2 (23) and Al_2O_3 (18) with heptamolybdate. It was found that with increasing potassium content polymolybdate species depolymerized progressively. At a K/Mo ratio of 2 the samples contained mainly K_2MoO_4 which was differently distorted than in crystalline K_2MoO_4. Impregnating SiO_2 with K_2MoO_4 led to spectra which indicated the formation of $MO_2O_7^{2-}$ species. Martin *et al*. (29) studied the structure of molybdenum oxocompounds formed in TiO_2-supported MoO_3 doped with different alkali metals. They have found that on the Li-doped catalyst only Li_2MoO_4 was observed, but on the K-doped sample octahedrally and tetrahedrally coordinated Mo were detected. It was proposed that $K_2Mo_2O_7$ was formed, because in the dimolybdate the anion has equal numbers of [MoO_4] tetrahedral and [MoO_6] octahedral units (29). In the present case, as Fig. 4 shows, the Raman spectra of K_2MoO_4 supported on SiO_2 did not change significantly; the catalyst contains mostly monomolybdate in the original structure.

On the Raman spectra of SiO_2-supported Rb_2MoO_4 a new shift was detected at 928 cm^{-1} while the intensity of the band at 885 cm^{-1} significantly decreased. This observation might indicate the formation of a new compound, dimolybdate, as was found in the case of potassium molybdate (9). The structure of dimolybdate contains Mo as mentioned above not only in tetrahedral coordination but in octahedral, too. A Raman band characteristic of the bending mode of the terminal Mo=O in the octahedral position is at about 291 cm^{-1} in $(NH_4)_2Mo_2O_7$ (20), but in this region no new band was observed. So we may suppose that the shift of

the Raman band from 885 cm^{-1} to 928 cm^{-1} could be due to the formation of a distorted [MoO_4] tetrahedron on the SiO_2 support. The wavenumber shift observed in the case of Rb_2MoO_4/SiO_2 means about 0.02 Å difference in the Mo–O band distance which can be calculated from the above-mentioned equation (20). By solid-state NMR it was found (30) that a modification of K_2MoO_4 contains highly distorted [MoO_4] tetrahedra with Mo–O distances differing by 0.04 Å. This observation also supported our suggestion that Rb_2MoO_4/SiO_2 can contain highly distorted tetrahedron.

In the case of cesium molybdate silica sample the Raman shifts were detected at 936, 912, and 218 cm^{-1}. These peaks can be assigned to dimolybdate species (12).

The temperature-programmed reduction of silica-supported alkali metal molybdates proceeds in practically the same temperature range as in the case of MoO_3/SiO_2; the reduction started above 773 K and the peak maximum of the TPR curve was at about 950 K (6). For the Li and Na salts, the reduction occurred in a narrow peak, while the main TPR curves of potassium, rubidium, and cesium molybdates proceeded by a small shoulder between 700 and 860 K. The onset of the reduction of the silica-supported alkali metal molybdates increased from cesium to lithium (6). The average valency of the molybdenum after completion of reduction in H_2 up to 1100 K was around 3 for potassium, rubidium, and cesium and 4 for lithium and sodium molybdates (6).

4.2. Possible Mechanism of the Methane Oxidation

In our previous studies (5, 6, 9) we supposed that the mechanism of methane and ethane oxidation on SiO_2-supported potassium molybdates can be described in terms of selective cycles which produce formaldehyde or acetaldehyde and in terms of nonselective cycles which yield carbon dioxide. In this case we can also presume that there is a selective route and a nonselective cycle for the methane conversion.

There is a general agreement that methane activation involves the removal of a hydrogen atom by surface O to give surface methyl groups.

Based on spectroscopic evidence Lunsford and coworkers (31, 32) assumed that the reaction is initiated by the formation of O^- on the Mo^{VI} sites of the surface. These ions are responsible for the H abstraction from CH_4 to form methyl radicals which react rapidly with the surface to form methoxy groups. This complex may then decompose to HCHO or react with water to form CH_3OH.

It was suggested (33) that terminal oxygen (Mo=O) promotes the formaldehyde production, while bridging oxygen (Mo–O–Mo) accelerates the deep oxidation of methane. Another assumption is (34) that the active species for formaldehyde formation are the well-dispersed molybdenum oxide clusters on SiO_2.

With regard to the oxygen species involved in the oxidation process we pointed out that the O^{2-} ions of molybdate react with methane under the experimental conditions as indicated by the formation of products following the interaction of methane with supported K_2MoO_4 (9) and with Rb_2MoO_4/SiO_2 in the absence of gaseous oxygen. In the case of K_2MoO_4/SiO_2, however, HCHO was not identified among the reaction products. This would suggest that in this case the lattice O^{2-} is not responsible for the selective route of methane oxidation; however, after the injection of CH_4 onto Rb_2MoO_4/SiO_2, HCHO formation was detected. It could be proposed that on the latter sample there are oxygen species which are effective in the HCHO formation. In the presence of O_2, either O_2 was added to CH_4 or CH_4 was injected into O_2, or $O_2 + CH_4$ pulses were injected into the sample, the HCHO formation was much higher (Fig. 7). This means that the adsorbed oxygen plays an important role in the activation of CH_4 and in the formation of methoxy species. Accordingly we propose the following steps for the selective oxidation:

$$CH_{4(g)} + O^-_{(s)} = CH_{3(s)} + OH^-$$

$$CH_{3(s)} + O^-_{(s)} = CH_{3}\text{-}O^-_{(s)}.$$

Methoxy species react further with OH^- ion to give formaldehyde:

$$2Mo^{6+} + CH_3 - O^- + OH^- = HCHO + 2Mo^{5+} + H_2O.$$

With regard to the CO_2 formation we have observed that when O_2 was injected (O_2 conversion 56%) into CH_4 a 2–3 times higher amount of CO_2 was formed than when CH_4 was added into O_2 (Fig. 7). These results suggest that when the CH_x fragment adsorbed on the surface reacts with O_2 it produces CO_2 to a much higher extent than when the CH_4 reacts with adsorbed oxygen. After treating the surface with $CH_4 + O_2$ (9 : 1) pulses the O_2 conversion was only about 20% and the amount of CO_2 was less by more than 1 order of magnitude than when O_2 was injected into the CH_4 stream. These results may support the idea that the surface activation of methane is slower than that of O_2.

In addition to the above reactions, the methyl groups formed on the surface may couple in the gas phase to give ethane:

$$2CH_3 = C_2H_6.$$

The subsequent total dehydrogenation of methyl groups may also occur. The presence of surface carbon was clearly documented when Rb_2MoO_4/SiO_2 was treated with CH_4. However, after the catalytic run, we found only a very small amount of surface carbon, so this route of CH_3 reaction in the presence of oxygen is negligible. The products of total oxidation, CO_2 and H_2O, could be the result of the direct oxidation of CH3 and/or HCHO.

During the catalytic run all the catalysts underwent significant deactivation, which was exhibited not only in the conversion of methane, but also in the rate of product

formation. This decay was much less in the formation of HCHO as indicated by the increase of the selectivity of this compound with the progress of the deactivation. The decrease in the catalyst activity cannot be attributed to the carbon deposition as we found very little carbon after the measurement which lasted for 3 h. We did observe, however, the partial reduction of the catalysts but the reduction degree of the sample cannot explain the activity decrease of the samples. By means of XP spectroscopy we observed a decrease in the Mo/Si ratio after the catalytic reaction, too. The activity loss of the alkali metal molybdate catalyst can be explained by the decrease in the amount of surface Mo atoms.

4.3. Comparison of the Catalytic Behavior of Alkali Metal Molybdates

From the comparison of the catalytic performance of alkali metal molybdates, we can state that the initial methane conversion increased with the size of the cations with the exception of Rb, i.e., in the sequence of Li, Na, K, Cs. This order corresponds well to the ease of the reduction of alkali metal molybdates (6), which supports the idea that the role of reduced sites in the formation of Mo^{6+}–O^- centers is important in the activation of methane.

The above-mentioned order will be somewhat different when the steady-state conversions are compared: $Rb_2MoO_4 > K_2MoO_4 > Cs_2MoO_4 > Na_2MoO_4 = Li_2MoO_4$ (Table 3), although the highest difference in the conversion with the exception of Rb_2MoO_4/SiO_2 between the other samples is below 20%.

When the consumption rate of methane is related to the Mo/Si ratio determined by XPS there is no systematic change as a function of the size of alkali metal ions. The specific rate in the presence of Na_2MoO_4 and Li_2MoO_4 is about the half that of MoO_3/SiO_2. These data agree well with the earlier finding that Li and Na additives decrease the activity of MoO_3 (11). Recently we found that the conversion of methane was almost the same when either potassium monomolybdate or potassium dimolybdate containing sample was the catalyst (9). These results suppose the present observation that the activity of the cesium molybdate sample containing mainly dimolybdate species is not higher than that of the other alkali metal molybdates.

The efficiency of Rb_2MoO_4/SiO_2 is at least 4 times higher than that of the other samples taking into account MoO_3/SiO_2, too. The rate of HCHO formation related to the surface Mo/Si ratio was also the highest in the case of Rb_2MoO_4/SiO_2. The high activity of this sample may be explained on the basis of the structure of the catalyst because we have found that the structure of Rb_2MoO_4/SiO_2 differs from those of the other silica-supported alkali metal molybdate samples. Namely, it turned out that Rb_2MoO_4/SiO_2 contains distorted [MoO_4] tetrahedra. In the other alkali metal molybdate catalysts the Mo ion is in the original tetrahedral or in the dimolybdate tetrahedral and octahedral coordination. This great difference in the structure of the samples can result in different behaviors of the catalysts. According to these results the outstanding activity of the Rb_2MoO_4/SiO_2 can be attributed to the distorted [MoO_4] tetrahedra of this catalyst.

ACKNOWLEDGMENTS

Financial support of this work by OTKA (contract number T 026340) is gratefully acknowledged.

REFERENCES

1. Foster, N. R., *Appl. Catal.* **19**, 1 (1985).
2. Fox, J. M., III *Catal. Rev.-Sci. Eng.* **35**, 169 (1993).
3. Spencer, N. D., *J. Catal.* **109**, 187 (1988).
4. Khan, M. M., and Somorjai, G. A., *J. Catal.* **91**, 263 (1985).
5. Erdőhelyi, A., Máté, F., and Solymosi, F., *Catal. Lett.* **8**, 229 (1991).
6. Erdőhelyi, A., Máté, F., and Solymosi, F., *J. Catal.* **135**, 563 (1992).
7. Kiwi, J., Thampi, K. R., and Grätzel, M., *J. Chem. Soc., Chem. Commun.* 1690 (1990).
8. Szőke, A., and Solymosi, F., *Appl. Catal. A: General* **142**, 361 (1996).
9. Erdőhelyi, A., Fodor, K., and Solymosi, F., *J. Catal.* **166**, 244 (1997).
10. Sexton, A. W., MacGiolla Coda, E., and Hodnett, B. K., *Catal. Today* **46**, 127 (1998).
11. Spencer, N. D., Pereira, C. J., and Grasselli, R. K., *J. Catal.* **126**, 546 (1990).
12. Banares, M. A., Spencer, N. D., Jones, M. D., and Wachs, I. E., *J. Catal.* **146**, 204 (1994).
13. Marchi, A. J., Lede, E. J., Requeja, F. G., Renteria, M., Irusta, S., Lombardo, E. A., and Miro, E. E., *Catal. Lett.* **48**, 47 (1997).
14. Retgers, J. M., *Z. Phys. Chem.* **8**, 6 (1891).
15. Romijn, G., *Z. Anal. Chem.* **39**, 60 (1900).
16. Rocchiccioli-Deltcheff, C., Amirouche, M., Che, M., Tatibouët, J.-M., and Fournier, M., *J. Catal.* **125**, 292 (1990).
17. Matsumoto, K., Kobayashi, A., and Sasaki, Y., *Bull. Chem. Soc. Jpn.* **48**, 1009 (1975).
18. Verbruggen, N. F. D., Mestl, G., von Hippel, L. M. J., Lengeler, B., and Knözinger, H., *Langmuir* **10**, 3063 (1994).
19. von Becher, H. J., *Z. Anorg. Allg. Chem.* **474**, 63 (1981).
20. Hardcastle, F. D., and Wachs, I. E., *J. Raman Spectrosc.* **21**, 683 (1990).
21. Driscoll, S. A., Gardner, D. K., and Ozkan, U. S., *J. Catal.* **147**, 379 (1994).
22. Kim, D. S., Segawa, K., Soeya, T., and Wachs, I. E., *J. Catal.* **136**, 539 (1992).
23. Verbruggen, N. F. D., von Hippel, L. M. J., Mestl, G., Lengeler, B., and Knözinger, H., *Langmuir* **10**, 3073 (1994).
24. Gatehouse, B. M., and Leverett, P., *J. Chem. Soc. A* 849 (1969).
25. Zachariasen, W. H., *Norsk. Geol. Tidsskr. B* 965 (1926).
26. Lindqvits, I., *Acta Chem. Scand.* 1066 (1950).
27. Kools, F. X. N. M., Koster, A. S., and Rieck, G. D., *Acta Crystallogr. B* **26**, 1974 (1970).
28. Gonschorek, W., and Hahn, Th., *Z. Kristallogr.* **138**, 167 (1973).
29. Martin, C., Martin, I., Rives, V., and Malet, P., *J. Catal.* **161**, 87 (1996).
30. Mastikhin, V. M., Lapina, O. B., and Maximovskaya, R. J., *Chem. Phys. Lett.* **148**, 413 (1988).
31. Liu, H. F., Liu, R. S., Liew, K. Y., Johnson, R. E., and Lunsford, J. H., *J. Am. Chem. Soc.* **106**, 4117 (1984).
32. Pak, S., Rosynek, M. P., and Lunsford, J. H., *J. Phys. Chem.* **98**, 11786 (1994).
33. Smith, M. R., and Ozkan, U. S., *J. Catal.* **141**, 124 (1993).
34. Suzuki, K., Hayakawa, T., Shimizu, M., and Takehira, K., *Catal. Lett.* **30**, 159 (1995).